Autonomous Precision Tracking and Docking of an Orbiter & Mars Sample Return Vehicle

Ching-Fang Lin
American GNC Corporation
9131 Mason Avenue
Chatsworth, CA 91311
Cflin@americangnc.com

Terry L. Huntsberger and Eric T. Baumgartner
Jet Propulsion Laboratory
4800 Oak Grove Drive
Pasadena, CA 91109
Terry.Huntsberger@jpl.nasa.gov
Eric.T.Baumgartner@jpl.nasa.gov

Abstract: This paper describes the design of a tracking and docking system for the Mars Sample Return Vehicle and Mars Orbiter. The design enables the implementation of efficient and stable maneuvering that allows the safe joining of two spacecraft. The accurate estimate of the relative motion between the two spacecraft leads to the generation of a smoothly varying and slowly traversed docking profile. The purpose of the paper is to present feature tracking in three dimensions utilizing a laser dynamic range imager and the control considerations that effect the execution of the commanded docking trajectory.

1 Introduction

One of NASA's main goals is autonomous missions to Mars. Planned future rock sampling visits involve, as a critical phase, a Mars Sample Return Vehicle docking with an Orbiter spacecraft encircling the planet. A successful docking procedure involves the generation of the proper trajectory until the final spacecraft interlock instance. The mission of a sampler is to perform far-space exploration and to bring materials from the Mars surface back to earth. Due to energy limitations, an optimal fuel trajectory is designed and the sampler is launched along this trajectory into a synchronous orbit to perform docking with an orbiter, as shown in Figure 1. From the point P1 to the point P2, the sampler is launched into a low Mars orbit (LMO). Then the sampler moves along the LMO from the point P2 to the point P3 without wasting additional energy. At the point P3, the sampler performs the orbit transfer maneuver and moves into a synchronous orbit of Mars where the Orbiter is located. After entering into a synchronous orbit, the sampler docks with the orbiter.

Due to the light structure characteristics of a sampler, a low impact docking approach is required. The docking process between a sampler and an orbiter is generally divided into three phases [9], as shown in Figure 2:

(1) The approach phase: From about 10Km to 500m. During this phase, the sampler motion is considered as that of a point mass. The sampler's attitude is ignored.
(2) The docking preparation phase: From about 500m to 2m. In this phase, the attitude controller is activated and gradually tunes the sampler attitudes with respect to the orbiter docking plane (rendezvous) and makes the relative attitude tend to zero when reaching the point S_2.
(3) The docking phase: within about 2m. The docking velocity is kept within a safe velocity, which is a very small velocity of about 1cm/s, in order to avoid a possible serious impact between the sampler and the orbiter when the docking is finished.

This paper mainly focuses on final docking phase. In order to perform high precision tracking and docking, LDRI (laser dynamic range imager) technology [5][6] is investigated and employed. Fuzzy logic based guidance and control scheme is proposed to accommodate environmental uncertainty. The related simulation results are presented.

2 LDRI based High Precision Tracking

An LDRI is one kind of scannerless imaging laser radar with high precision ranging. An LDRI tracker, as shown in Figure 8, is implemented to provide the accurate position of a pattern of points, which are used to determine the relative attitude between the sampler and the orbiter. It also tracks a pattern of selected points on the orbiter, derived from the LDRI image, without loss of tracking. One frame of LDRI image data consists of two image data, one is a reflectance image and the other a range image. The range image contains the range data for each pixel in the reflectance image. The reflectance image is used for image object (pattern or feature) tracking.

During the docking process, the accuracy of the relative position and attitude plays a key role that determines the docking success or failure. As mentioned above, the docking is actually initiated at the point S_1, as shown in Figure 2. At this stage, the LDRI tracker is used to obtain the accurate relative position and attitude between the sampler and the orbiter. The docking activation distance, i.e., the point S_1, away from the orbiter is determined by the LDRI tracker and the LDRI sensitivity.

In Figure 3, the coordinate system $X_rY_rZ_r$ denotes the orbiter docking plane coordinate system, the coordinate system $X_dY_dZ_d$ denotes the sampler docking plane coordinate system, the coordinate system $X_cY_cZ_c$ denotes the LDRI coordinate system, and the coordinate system $X_sY_sZ_s$ denotes the sampler body coordinate system. The required docking relative position and attitude depend on the coordinate systems $X_rY_rZ_r$ and $X_dY_dZ_d$. The relative position and attitude measurements are given in the coordinate system $X_cY_cZ_c$. The motion control and attitude control are implemented in the coordinate system $X_sY_sZ_s$. Therefore the transformation among these coordinate systems is investigated and established to implement autonomous precision tracking and docking between the sampler and the orbiter.

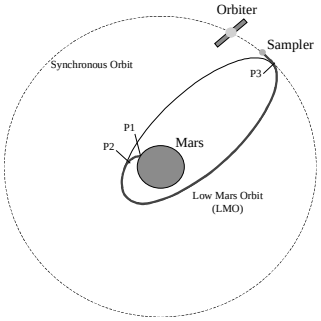

Figure 1 The Return Trajectory for a Mars Sample Return Mission

The attitude of each docking plane consists of three angles: pitch (θ), yaw (ϕ), and roll (γ). When the relative attitude between the two docking planes tends to zero, it makes the two docking planes parallel to each other. Another image orientation angle of the docking plane is required to complete docking. The image is specially designed to assure the required docking accuracy.

For a given pixel (i, j) in an LDRI reflectance image, the corresponding Cartesian coordinates are:

$$x = R \cdot i \Big/ \sqrt{i^2 + j^2 + f^2} \qquad (2.1a)$$

$$y = R \cdot j \Big/ \sqrt{i^2 + j^2 + f^2} \qquad (2.1b)$$

$$z = R \cdot f \Big/ \sqrt{i^2 + j^2 + f^2} \qquad (2.1c)$$

where R is the range data directly obtained from the corresponding range image and f is the focal length for the current frame of the LDRI image. (x, y, z) also denotes the relative position of a target with respect to the LDRI lens. If the distance between two tracking points is known, the current focal length can be obtained from the following expression:

$$\frac{i_1 i_2 + j_1 j_2 + f^2}{\sqrt{i_1^2 + j_1^2 + f^2}\sqrt{i_2^2 + j_2^2 + f^2}} = \frac{R_1^2 + R_2^2 - D^2}{2R_1R_2}$$

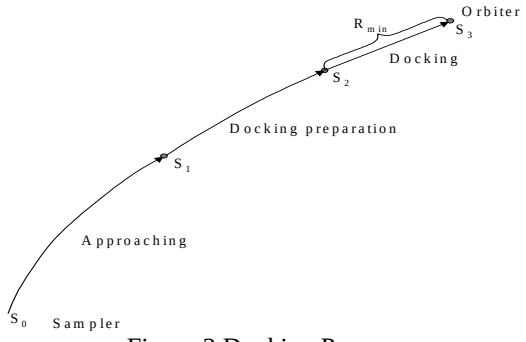

Figure 2 Docking Process

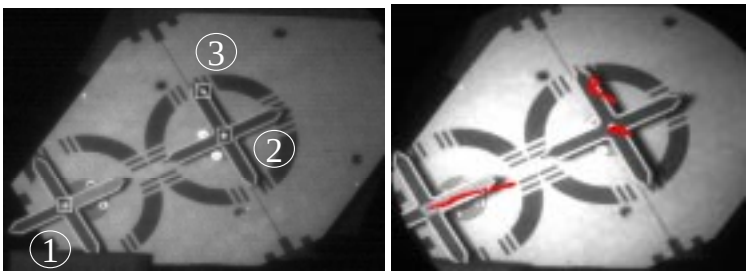

(a) (b)

Figure 4 The selected tracking points

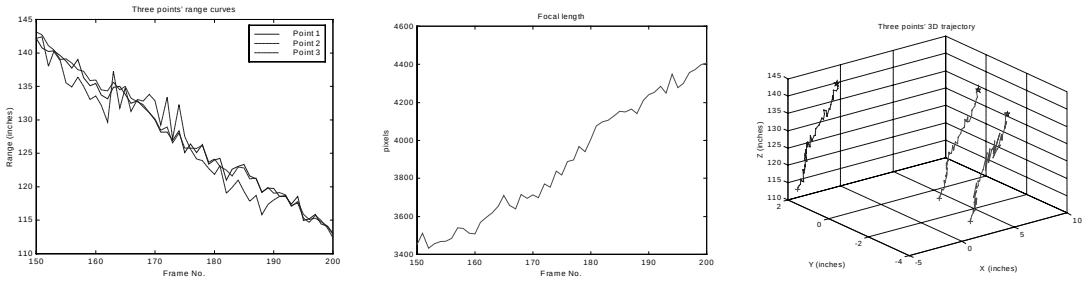

(a) (b) (c)

Figure 5 Results of range, focal length, and 3D trajectory

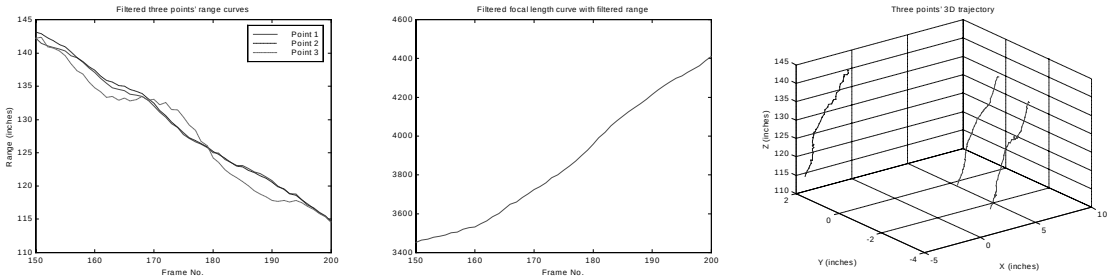

(a) (b) (c)

Figure 6 The results of range, focal length, and 3D trajectories based on Kalman filter

(2.2)

where (i_1, j_1) and (i_2, j_2) are the image coordinate values of two selected points P_1 and P_2, R_1 and R_2 denote the corresponding range data of these two points, and *D* denotes the distance between these two points.

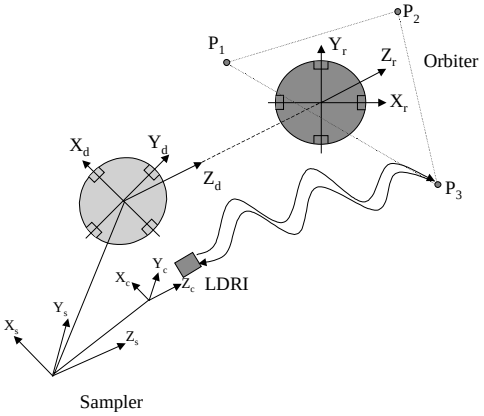

Figure 3 The Coordinate Systems Relationship between a Sampler and an Orbiter

The target used for testing is a Double Cross Target (DCT) from NASA Johnson Space Center. Three points are selected on two double crosses, as shown in Figure 4(a), at the 150th frame. Figure 4(b) shows the motion trajectories of three tracking points from the 150th frame to 200th frame. The range curves of these three points are shown in Figure 5(a). The distance between point 1 and point 2 is 8 inches. The focal length and 3-dimensional relative position curves obtained according to Eq.(2.1) and Eq.(2.2) are shown in Figure 5(b) and 5(c), respectively.

3 Kalman Filter for High-Precision Tracking with LDRI Imagery

LDRI imagery and image processing technologies allow for tracking in 3-dimensions. Kalman filtering techniques can thus be utilized to improve the tracking accuracy. Kalman

filtering is a model-based estimation technique, which is ideally suited for docking applications. The closing velocities between the mother satellite and the resupply satellite are very slow during docking. Such a motion is well defined using an appropriate acceleration model.

The benefits of introducing a Kalman filter into LRDI tracking, which is formulated in 3D world coordinates, entail two aspects. First, Kalman filtering and smoothing improve the tracking accuracy based on a motion dynamics formulation, which makes subpixel accuracy feasible. Second, a Kalman filter can be used to predict the 3D coordinates of a point of interest in the next frame from the current 3D coordinates. Such a prediction can be used to determine the center and size of the search window for the tracking algorithm.

The latter is very important for the tracking algorithms. Proper location and size of the search window are crucial for successful tracking. An incorrect location or too small a size of the search window will definitely lead to loss of track. If the search window is chosen too large, more computation is needed to carry out the cross plane correlation. By incorporating the target 3D position into the Kalman filter states, the state estimate can be used to determine the center of the search window in image coordinates, and the state estimate covariance matrix can be used to determine the size of the search window in image coordinates.

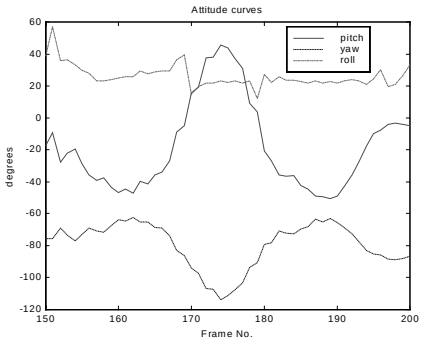

Figure 7 Attitude curves

Based on the Kalman filter technology, the new range data, focal length, and 3D trajectory curves are shown in Figure 6(a), 6(b), and 6(c), respectively. Compared with the results in Figure 5, the results in Figure 6 are much smoother. The attitude results obtained according to the range, the focal length, and the relative position in Figure 6, are shown in Figure 7.

4 Control System Design

Motion Equations

According to the Clohessey-Wiltshire equations, the linearized relative motion equations of the sampler and the orbiter are

$$\begin{aligned} \ddot{x} - 2\omega_0 \dot{z} - f_x &= u_x \\ \ddot{y} + \omega_0^2 y - f_y &= u_y \\ \ddot{z} + 2\omega_0 \dot{x} - 3\omega_0^2 z - f_z &= u_z \end{aligned} \qquad (4.1)$$

where x, y, z is the position of the sampler in the coordinate frame ($\hat{x}\hat{y}\hat{z}$) with the orbiter at the origin, ω_0 is the orbit rate, and f_x, f_y, and f_z are the components of the uncertain environmental disturbances $\vec{f}$. u_x, u_y, and u_z are the components of the control forces in the coordinate frame ($\hat{x}\hat{y}\hat{z}$).

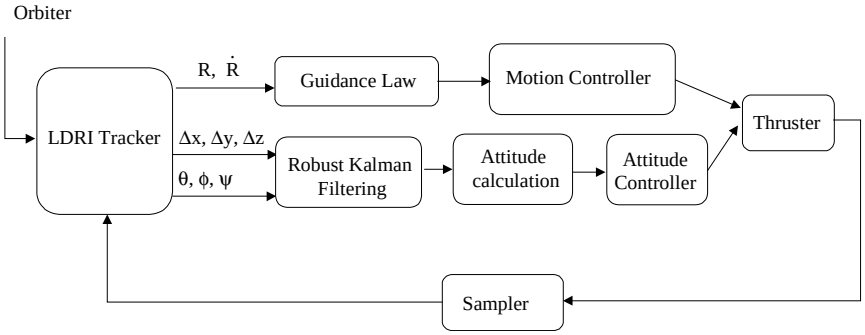

Figure 8 Autonomous Precision and Docking System

Control System Architecture

Given a desired position trajectory $q_d(t)$ for the sampler, with respect to the orbiter, the primary objective of the sampler control system at the first phase (approach phase) is to design the control input u_f such that $q(t) \rightarrow q_d(t)$ as $t \rightarrow \infty$, i.e., to make the position tracking error tend to zero. The position tracking error is defined as

$$e(t)=q_d(t)-q(t)$$

and a filtered tracking error is designed as

$$e_f(t) = \dot{e}(t) + \Lambda e(t)$$

to make the sampler's dynamic characteristics have good damping.

At the preparation of the docking phase, the objective of the sampler's control system is to align the two planes in parallel and for the relative position errors in the x and y axes to tend to zero at the point S_2 and the relative distance in the z axis to be within the required minimum docking distance with a desired docking velocity.

A z-approach method is designed to complete docking, i.e., now the relative attitude and orientation of the two docking planes are locked. The docking velocity is accurately controlled based on the LDRI precision ranging.

The sampler's guidance and control system block diagram is shown in Figure 8. It consists of a motion control loop and an attitude control loop. The motion controller performs the trajectory control, i.e., the relative position tuning between the sampler and the orbiter, according to the guidance law and the trajectory error. A robust Kalman filter is used to estimate the state variables, as required for relative attitude calculation.

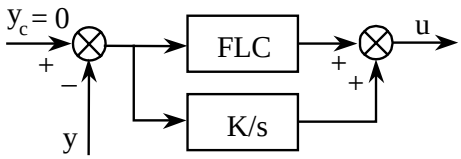

Figure 9 FLC+Integral scheme

Fuzzy logic control plus integral scheme

From the open loop characteristics of the relative motion dynamics Eq.(4.1) between two targets in a circular or near-circular orbit, an external or initial disturbance causes the deflection drifts. A new kind of motion control scheme, i.e., fuzzy logic control plus integral (FLC+I) scheme, is proposed as shown in Figure 9. In this new scheme, an integrator is introduced to eliminate the stable error and an FLC module is introduced to eliminate the system parameter uncertainty and environmental uncertain disturbances. Figure 10 shows the relative position, control output, and 3D trajectory by employing the proposed FLC+I motion control scheme.

5 Conclusions

In this paper, an LDRI based guidance and control scheme is proposed for high precision docking in the Mars Sample Return mission. The Kalman filter technique has been successfully applied in the determination of relative position and attitude based on the LDRI image data from the simulation results. A FLC+I motion control scheme has also been proposed in this paper and a satisfied performance of relative motion control during docking has been achieved.

Acknowledgment

The authors are grateful to Dr. George Studor of NASA Johnson Space Center for his support during the course of this study.

References

[1] Lin, C.F., **Modern navigation, guidance, and control processing**. Englewood Cliffs, New Jersey, Prentice-Hall, 1990.

[2] Lin, C.F., **Advanced control system design.** Englewood Cliffs, New Jersey, Prentice-Hall, 1993.
[3] Huntsberger, T.L. and S.N. Jayaramamurthy, **Determination of the optic flow field using the spatiotemporal deformation of region properties**, *Pattern Recognition Letters*, 6 (1987), pp. 169-177
[4] Huntsberger, T.L. and S.N. Jayaramamurthy, **Determination of the optic flow field in the presence of occlusion**, *Pattern Recognition Letters*, 8 (1987), pp. 325-333
[5] George Studor, **Laser Dynamic Range Imager Space Shuttle Flight Demonstration**, NASA JSC, Houston, TX 77058, Structural Mechanics Report (1998)
[6] Schmitt, R.L., R.J. Williams, and J.D. Matthews, **High frequency scannerless imaging laser radar for industrial inspection and measurement applications**, Sandia Report, SAND96-2739 UC-906, 1996.
[7] Clohessey,W.H. and R.S. Wiltshire, **Terminal guidance system for satellite rendezvous**, *Journal of the Aerospace Sciences*, vol.27(9), 1960, pp.653-658,674
[8] Pappa, R.S., M.G. Gilbert, and S.S. Welch, **Simulation of the Photogrammetric Appendage Structural Dynamics Experiment**, *Proceedings of the 14th IMAC*, Dearbon, MI, pp.873-879, 1996.
[9] Kawano, I., M. Mokuno, T. Kasai, and T. Suzuki, **Result and Evaluation of Autonomous Rendezvous Docking Experiments of ETS-VII**, 1999 AIAA Guidance, Navigation, and Control Conference and Exhibit, AIAA-99-4073, 1999

[2] Lin, C.F., **Advanced control system design.** Englewood Cliffs, New Jersey, Prentice-Hall, 1993.
[3] Huntsberger, T.L. and S.N. Jayaramamurthy, **Determination of the optic flow field using the spatiotemporal deformation of region properties**, *Pattern Recognition Letters*, 6 (1987), pp. 169-177
[4] Huntsberger, T.L. and S.N. Jayaramamurthy, **Determination of the optic flow field in the presence of occlusion**, *Pattern Recognition Letters*, 8 (1987), pp. 325-333
[5] George Studor, **Laser Dynamic Range Imager Space Shuttle Flight Demonstration**, NASA JSC, Houston, TX 77058, Structural Mechanics Report (1998)
[6] Schmitt, R.L., R.J. Williams, and J.D. Matthews, **High frequency scannerless imaging laser radar for industrial inspection and measurement applications**, Sandia Report, SAND96-2739 UC-906, 1996.
[7] Clohessey,W.H. and R.S. Wiltshire, **Terminal guidance system for satellite rendezvous**, *Journal of the Aerospace Sciences*, vol.27(9), 1960, pp.653-658,674
[8] Pappa, R.S., M.G. Gilbert, and S.S. Welch, **Simulation of the Photogrammetric Appendage Structural Dynamics Experiment**, *Proceedings of the 14th IMAC*, Dearbon, MI, pp.873-879, 1996.
[9] Kawano, I., M. Mokuno, T. Kasai, and T. Suzuki, **Result and Evaluation of Autonomous Rendezvous Docking Experiments of ETS-VII**, 1999 AIAA Guidance, Navigation, and Control Conference and Exhibit, AIAA-99-4073, 1999

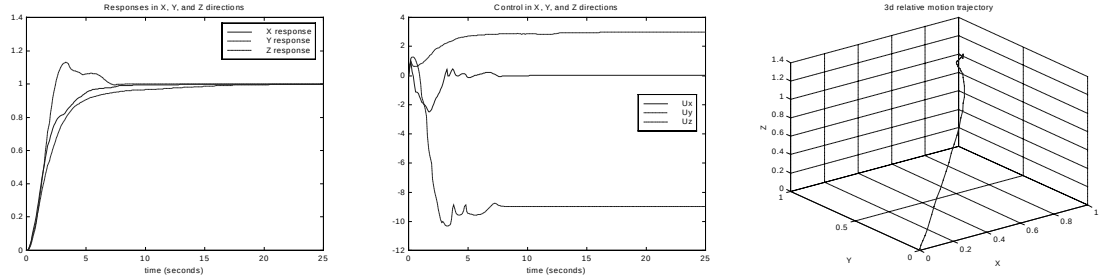

(a) (b) (c)

Figure 10 Simulation results